A New Nuclear Medicine Scintillation Camera Based on Image-Intensifier Tubes

H. Mulder and E. K. J. Pauwels

N.V. Optische Industrie "de Oude Delft," Delft, and Leyden University Hospital, Leyden, The Netherlands

A large-field scintillation camera for nuclear medicine application has recently been developed by Old Delft. The system is based on a large-field image-intensifier tube preceded by a scintillator mosaic. A comparison is made with present state-of-the-art scintillation cameras in terms of modulation transfer function (MTF) and sensitivity. These parameters, which determine the performance of scintillation cameras, are not independent of each other. Therefore, a comparative evaluation should be made under well-defined and identical conditions. The new scintillation camera achieves considerable improvement in image quality. In fact, the intrinsic MTF of the new camera is rather close to unity in the spatial frequency range up to 1 line pair per centimeter (lp/cm). Further improvement would require a fundamentally new approach to gamma imaging, free of the limitations of conventional collimators (e.g., coded-aperture imaging techniques).

J Nucl Med 17: 1008–1012, 1976

This paper describes a new nuclear medicine scintillation camera, based on image-intensifier tubes, and reports early results obtained with this device in clinical practice at the Leyden University Hospital.

THEORETICAL CONSIDERATIONS

However, let us first explain why our efforts to improve image quality over that of present scintillation-camera systems are worthwhile from a physical point of view. We feel that further improvement may be expected only by way of some fundamentally new approach to gamma-photon imaging, such as Fresnel zone plates (*1,2*). Signal-to-noise problems may limit the clinical value of Fresnel zone plate systems with large fields (*3*). To draw conclusions about dot-density differences observed in a scintigram, statistical considerations must be taken into account. Present state-of-the-art techniques involve recording densities of about 400 scintillations per square centimeter in the object. With this information density, there is a 33% probability that 1-cm^2 details may show a nonsignificant noise contrast of 5% or more from random fluctuations alone. In fact, perception of 1-cm^2 details in typical contrast ranges represents the limit of present scintillation cameras.

Increasing the resolution by a factor of 2 requires a fourfold increase in the number of scintillations recorded from a 1-cm^2 object in order to obtain the same signal-to-noise ratio. Unfortunately, in order to achieve this improved resolution the collimator would have one-fourth of its former sensitivity. This would require a 16-fold increase in activity or exposure time, which is not acceptable in most practical cases. Therefore, a more practical approach to the development of a scintillation camera would be to strive for the improvement of the modulation transfer function (MTF) in order to increase the signal-to-noise ratio in the frequency range of interest, rather than trying to extend that

Received Dec. 16, 1975; revision accepted June 2, 1976.

For reprints contact: E. K. J. Pauwels, Academisch Ziekenhuis Leiden, Rijnsburgerweg 10, The Netherlands.

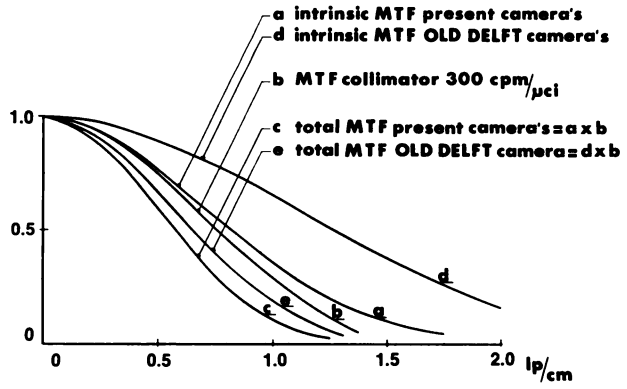

FIG. 1. Various relevant MTF curves. See text.

frequency range. Though the theoretical considerations are beyond the scope of this paper, we feel accordingly that interchanging collimators should be practiced more commonly in gamma imaging. Engineering efforts should be directed toward simplifying collimator changing or to the development of "adjustable" collimators.

In Fig. 1 we show the improvement achieved in intrinsic MTF with our system as compared with currently available scintillation cameras. These cameras, now recognized as practical diagnostic instruments in nuclear medicine, are predominantly of the Anger type (*4*). However, they seem to have reached almost the maximum performance achievable. Only a considerable increase of the number of photomultipliers or a substantial improvement of the sensitivity of the photocathodes could improve their performance further (*5*).

Curve a of Fig. 1 represents the intrinsic MTF of the best scintillation cameras now available, expressed as a function of spatial frequency, corresponding to a full width half maximum (FWHM) of 0.6 cm for the line spread function and to an intrinsic resolution of about 1.7 line pairs per centimeter (lp/cm). This last figure corresponds to a 0.3-cm spacing in a lead bar phantom. Curve b is the MTF of a commonly used parallel-hole collimator, having a sensitivity of 300 cpm/μCi at an object distance of 10 cm. These curves are valid for 140-keV photons. Curve c is the total MTF of the complete camera, obtained by multiplying curves a and b. The resulting resolution is about 1.1 lp/cm for high-contrast objects at a distance of 10 cm. Curve d is the intrinsic MTF of our scintillation camera, which up to 1.0 lp/cm is rather close to the maximum achievable, making efforts to improve just the MTF further hardly worthwhile. In those cases in which the activity administered or the exposure time is not critical, a very-high-resolution collimator could bring the MTF close to curve d for the complete system. This represents a remarkable improvement over the situation illustrated in curve a. Curve e is the total MTF of our system with a limited amount of radioactivity and exposure time, obtained by multiplying curve d by curve b. A considerable improvement in MTF over curve c is obtained, although the resolution shows only a modest increase from 1.1 to about 1.3 lp/cm. Of greater importance, with objects having spatial frequencies of 1–1.3 lp/cm, the signal-to-noise ratio and probability of observing details are substantially improved, in some instances more than doubled. This result is of considerable clinical significance, especially when very small objects with high contrast, such as intraocular lesions, must be detected (*6*). Finally, we stress that with the better overall MTF of our scintillation, patient immobility becomes even more important in order to benefit fully from the improved image quality. Special equipment to immobilize the patient or to compensate for such movement is worth developing.

THE FIRST EXPERIMENTAL CAMERA

We developed two basically similar systems. They differ only with respect to the design of the scintillation mosaic and photocathode window of the large image-intensifier tube. Similar systems based on image-intensifier tubes have been previously developed by others (*7,8*).

Our first system had a useful detection area 30 cm in diameter. Its evaluation was carried out in actual practice at Leyden University in 1974. For mechanical reasons it could be used only in the vertical position. Figure 2 shows a schematic layout for this system. On the left is the parallel-hole collimator, which has 5,000 apertures. Behind each aperture is a scintillation crystal. These crystals, coated with a white reflective layer, are in optical continuity with the photocathode of a large image-intensifier tube. The useful diameter of the photocathode is 30

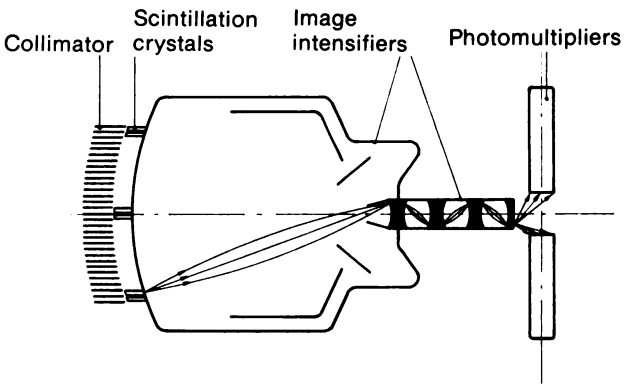

FIG. 2. Schematic layout of image-intensifier scintillation camera.

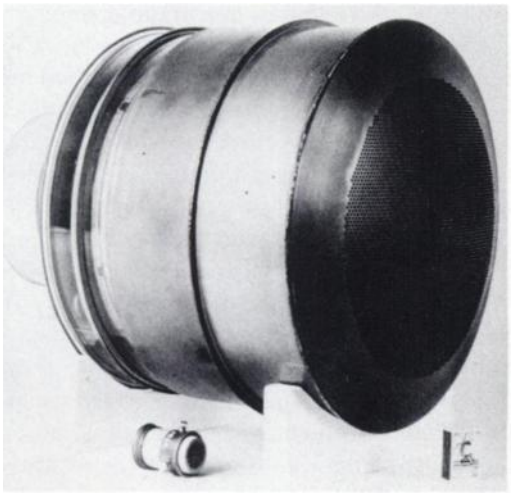

FIG. 3. Large-field image-intensifier tube with metal framework having 5,000 holes.

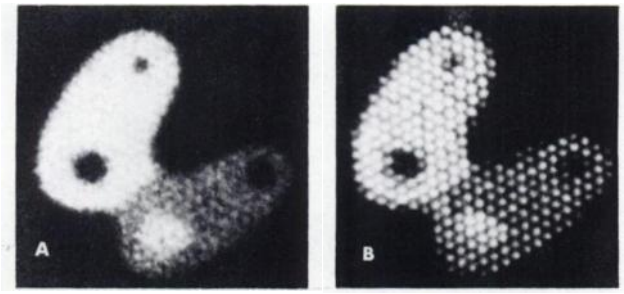

FIG. 4. Scintigram of thyroid phantom with phantom movement (A) and without (B).

cm. The demagnification of this tube is 12. Behind it are three smaller tubes, coupled to each other by fiberoptics, bringing the total light gain to about 2,000. The photocathode window of the large tube consists of a metal plate having 5,000 holes for the individual crystals; a 1-mm-thick glass window is fused to the plate. This framework serves as a support for the delicate glass window. In fact, it was the mechanical problems involved that limited the number of holes in this experimental camera. Because of the thinness of the glass window, the light spots produced on the photocathode by the crystals, although only 0.4 cm apart, are sufficiently well defined so that their images on the anode screen remain distinct. Nonuniformity of the individual crystals can be compensated to some extent by applying a photographic filter to this last screen; this is also used to compensate for photocathode and anode-screen nonuniformities.

When a gamma photon is absorbed by a scintillation crystal, the corresponding image on the last anode provides a light flux of intensity proportional to the energy of the photon. This light flux is largely collected by the photocathodes of four photomultiplier tubes, of which only two are shown. The electric signals produced by the photomultipliers are used to determine the pulse amplitude and the x and y coordinates of the gamma event. When the pulse height lies between the lower and upper levels of the preselected energy window, the scintillation is displayed in the correct position on a cathode-ray tube. The complete scintigram is obtained by photographing the screen of the tube over a pre-established exposure time.

Our system is fundamentally different from the Anger principle in that the various physical events involved (the gamma-to-scintillation conversion and the determination of the location and intensity of the scintillation) no longer take place within and around one common large-sized scintillation crystal coupled to numerous photomultipliers. Instead we achieve a functional and geometric separation of these events. On the one hand, this provides an opportunity to use a mosaic of small crystals, so that the geometric resolution can be improved by choosing smaller dimensions of the individual detector crystals. On the other hand, by using a demagnifying stage and subsequent light-amplifying imaging stages for the intensification of the individual scintillations, the system can determine their location and intensity more accurately with only four photomultipliers. Figure 3 shows the large image-intensifier tube and one of the smaller intensifiers.

To smooth out the mosaic effect of the scintillation crystal pattern, the patient was moved, during exposure, in a small circular path, 7.5 mm in radius, at right angles to the detector axis. This movement of each point in the patient was compensated electrically by an opposite movement of the image on the screen of the scope. Figure 4 illustrates this smoothing process with a scintigram made with a thyroid phantom. The scintigram on the right was taken with the phantom stationary. The resolution is so good that individual crystals, with their 4-mm separation, can be observed distinctly. The scintigram on the left is made with phantom movement, which, in addition to the smoothing effect, also improves the MTF and the resolution to some extent. To anticipate the actual clinical results, a skeletal scintigram of a rat is shown in Fig. 5. This image shows good resolution of the anatomic parts of the knee joint.

THE SECOND SCINTILLATION CAMERA SYSTEM

Our second scintillation camera has a useful detection area 36 cm in diameter. The mosaic of scintillation crystals consists of three hundred 2 × 2-cm blocks, each containing 25 crystals, 1 cm long and with 4 × 4-mm square faces. For this system we no

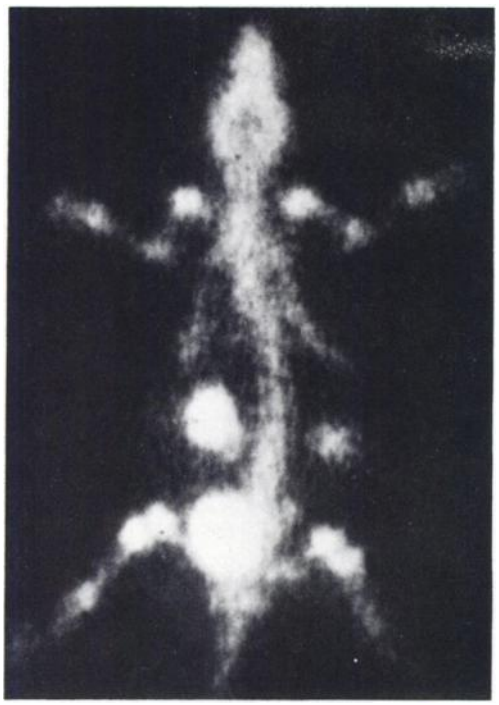

FIG. 5. Skeletal scintigram of rat.

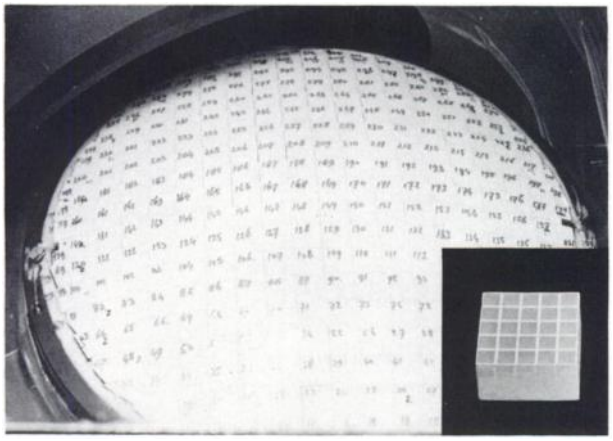

FIG. 6. Blocks mounted on exterior of cathode window. Inset: Block containing 25 coated scintillation crystals.

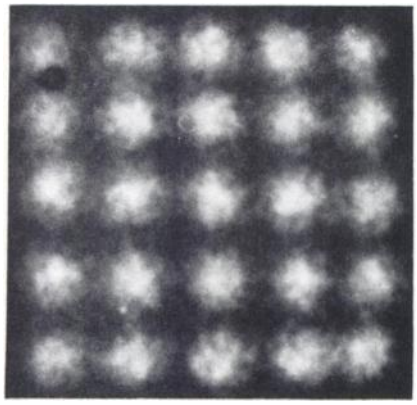

FIG. 7. Image of crystal block, photographed from scope.

longer have to use special multihole collimators providing one-to-one matching with the crystal pattern. Therefore, in our preliminary experiments we used a 25,000-hole collimator. The inset in Fig. 6 shows such a block, coated with a white reflective layer that also helps to exclude moisture. Figure 6 shows the 300 blocks mounted on the exterior of the input window of the large image-intensifier tube. The production costs for the whole scintillator were substantially lower than for the first experimental camera. More importantly, the individual differences in light output and energy resolution are smaller.

Last but not least, it is simple and not too expensive to make longer crystals, up to 2.5 cm, substantially improving the efficiency for higher photon energies. The input window of the large intensifier tube, without metal framework, is 0.5 cm thick. Consequently, the images of the individual crystals overlap, and the photographic filter on the last anode compensates only for the nonuniformity of the image-intensifier tubes and not for individual crystal differences. Moreover, because of the improved uniformity of the crystals, we have succeeded in obtaining an energy resolution of better than 20% for the complete camera. The overlapping of the crystal images does not seriously degrade the intrinsic MTF of the system, because the four-photomultiplier system determines the location of "the center of gravity" of each light spot (*9*). The FWHM Δx of the line spread function determined by the photomultipliers can be written as:

$$\Delta x^2 = \frac{k_1}{N_0} + \frac{k_2}{n_0}\Delta s^2,$$

in which the k_1 and k_2 are system constants, n_0 is the average number of photoelectrons released from the first photocathode, Δs is the FWHM of the light spot on that photocathode, and N_0 is the average number of photons emitted by the last anode screen. Although Δs is about 0.8 cm, due to crystal size and photocathode window thickness, we find a FWHM Δx of almost 0.25 cm for each crystal at 140-keV photons.

Figure 7 shows the image of a scintillation-crystal block, photographed from the scope, and it confirms the measured FWHM value. With the collimator, however, in practice the finite size of the individual crystals introduces an additional decrease in sharpness, which must be taken into account. This effect, expressed as an MTF multiplied by the Gaussian MTF of the four-photomultiplier system, leads to the overall non-Gaussian MTF of curve d in Fig. 2. This corresponds to a Gaussian line spread function with about 0.4 cm FWHM. The calculated curve is found to agree with the limiting intrinsic

resolution of almost 2.5 lp/cm, corresponding to a 0.2-cm spacing in a lead bar phantom.

To accomplish the smoothing of the crystal pattern, which we found desirable in our first system, we move the detector assembly in our second system rather than the patient, using a similar circular path of 7.5 cm radius. This movement can be employed in all positions of the camera head, making the system highly versatile. The clinical performance of the Old Delft camera is currently under test in our institution.

ACKNOWLEDGMENTS

The authors wish to thank Dr. Byck, a guest from Santa Rosa, California, for his outstanding help in preparing the manuscript. This paper was presented at the 3rd Congress of the European Association of Radiology, held in Edinburgh in 1975.

REFERENCES

1. BARRETT HH: Fresnel zone plate imaging in nuclear medicine. *J Nucl Med* 13: 382–385, 1972

2. BARRETT HH, HORRIGAN FA: Fresnel zone plate imaging of gamma rays. Theory. *Appl Opt* 12: 2686–2702, 1973

3. BARRETT HH, DE MEESTER GD: Quantum noise in Fresnel zone plate imaging. *Appl Opt* 13: 1100–1109, 1974

4. ANGER HO: Scintillation camera. *Rev Sci Instrum* 29: 27–33, 1958

5. TANAKA E, HIRAMOTO T, NOHARA N: Scintillation cameras based on new position arithmetics. *J Nucl Med* 11: 542–547, 1970

6. PAUWELS EKJ, VAN DIJK RA: Scintigraphy of intraocular lesions with Tc–Fe–ascorbic acid complex. A study on the radionuclide accumulation in malignant melanoma. In *Proceedings of the First International World Conference of Nuclear Medicine*. Tokyo, 1974, pp 716–719

7. HINE GJ, SORENSON JA: Image intensifier cameras. In *Instrumentation in Nuclear Medicine*. New York, Academic, 1974, pp 46–49

8. CONRAD B, PLATZ W: Das Scinticon, eine neue Gamma-Kamera. *Electro Medica* 4–5: 220–225, 1973

9. ROUX G, GAUCHER JC, LANSIART A, et al.: Détecteur photoélectronique analogique de la position de scintillations faiblement lumineuses. In *Photo-Electronic Image Devices*. New York, Academic, 1972, pp 1017–1029